Recent advances and applications of artificial intelligence in 3D bioprinting

Hongyi Chen[a,b], Bin Zhang[c*], Jie Huang[b*]

[a] Department of Computer Science, University College London, London, UK

[b]Department of Mechanical Engineering, University College London, London, UK

[c] Department of Mechanical and Aerospace Engineering, Brunel University London, London, UK

*Corresponding authors

bin.zhang@brunel.ac.uk

jie.huang@ucl.ac.uk

Contents

Abstract

3D bioprinting techniques enable the precise deposition of living cells, biomaterials and biomolecules, emerging as a promising approach for engineering functional tissues and organs. Meanwhile, recent advances in 3D bioprinting enable researchers to build in vitro models with finely controlled and complex micro-architecture for drug screening and disease modelling. Recently, artificial intelligence has been applied to different stages of 3D bioprinting including medical image reconstruction, bioink selection and printing process with both classical AI and machine learning approaches. The ability of AI to handle complex datasets, make complex computations, learn from past experiences, and optimize processes dynamically makes it an invaluable tool in advancing 3D bioprinting. The review highlights the current integration of AI in 3D bioprinting and discusses future approaches to harness the synergistic capabilities of 3D bioprinting and AI for developing personalized tissues and organs.

Keywords: 3D bioprinting; hydrogel materials; artificial intelligence; machine learning.

1. Introduction

The shortage of organs for transplantation is a global problem that has been around for decades. Meanwhile, ethical considerations regarding animal experimentation are always a concern and the use of alternatives to in vivo testing is needed. 3D printing and artificial intelligence (AI) technologies have emerged to profoundly impact humanity. 3D bioprinting, a 3D printing technique which involves layer-by-layer precise processing of bioink consisting of cells and biomaterials, has emerged as a promising biofabrication method [1, 2]. It has the advantages of cell encapsulation and precise spatiotemporal control of tissue scaffolds with desired composition, architecture and cell density which greatly increases the level of biomimicry of the cell niche [3]. 3D bioprinting could fabricate complex structures customizable to each patient and personalized medicine and provide a highly relevant biological systems and less invasive model in the laboratory for systemic investigations and evaluations. The extrusion-based, inkjet, and laser-assisted bioprinters are among the bio-fabrication methods that fabricate heterogeneous cell-laden structures such as kidney, heart, and cancer tissue mimics [4, 5].

3D bioprinting significantly enhances the fields of tissue/organ regeneration and in vitro model testing by utilizing its capabilities in precision, customization, and scalability [6]. In tissue and organ regeneration, bioprinting allows for the creation of complex, functional tissue constructs with well-defined architectures, improving their viability and integration within the body. This technology is essential for developing advanced organoids and large-scale tissue replacements [7, 8]. For in vitro model testing, 3D bioprinting is capable of producing of highly accurate and patient-specific models that mimic the architecture and functions of human tissues. This progresses the current in vitro models from a static 2D mono-layer culture towards dynamic and 3D culture systems, such as microbeads, organoids, and more recently 4D structures [9, 10]. These customized models are invaluable for precise drug testing and the development of personalized treatment strategies, offering a more relevant and efficient pathway from research to clinical application [11].

The capacity of AI to manage intricate datasets, perform complex computations, automate processes, learn from historical data, and dynamically optimize operations renders it an indispensable tool in advancing 3D bioprinting. It has been used in different stages of 3D bioprinting including medical image reconstruction, bioink selection and printing process with two approaches, classical AI and machine learning. The classical AI approach has been used to automate medical image reconstruction

at the designing phase of bioprinting, build intelligent printing systems capable of *in situ* printing on complex surfaces or defect sites of patients, and auto-adjusting printing parameters in real-time. Machine learning, capable of learning from big data for making predictions and finding patterns, has been used to optimize image processing and diagnosis, guide bioink selection, and optimize printing parameters.

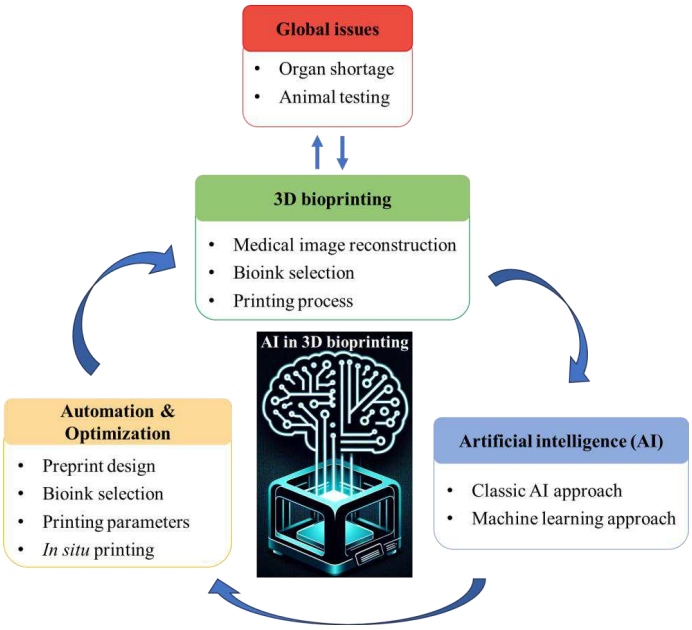

Figure 1 The schematic of 3D bioprinting and AI application in regenerative engineering.

This review explores 3D bioprinting techniques and bioinks for tissue and organ engineering, examines the current role of artificial intelligence in 3D bioprinting, and discusses future perspectives and solutions to harness the combined potential of 3D bioprinting and AI for creating tissues and organs for the global needs.

2. 3D bioprinting

2.1. 3D bioprinting technique

Bioprinting techniques can be classified by several criteria, including the stimuli applied for bioink deposition, the type of bioink deposition from the reservoir (orifice-free or orifice-based), and the printing modality (drop-based or extrusion-based) [3, 12]. This review centers on bioprinting technologies involving stimuli-responsive depositions, categorized into three categories: inkjet bioprinting (using thermal and

piezoelectric effects), extrusion-based bioprinting (utilizing air pressure or mechanical forces), and laser-assisted bioprinting (harnessing light energy). Figure 2 depicts the various types of 3D bioprinting technologies and their standard workflows for therapeutic applications.

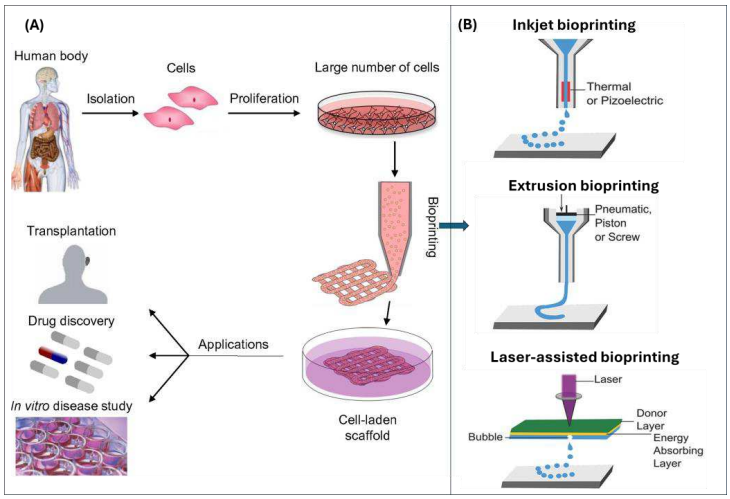

Figure 2. (A) The typical bioprinting workflow for therapeutic applications involves isolating and expanding human cells, printing cell-laden scaffolds, and using these scaffolds for therapy, drug testing, or disease modelling. C. Mandrycky, et al. Biotechnol. Adv., 34, 422-434, 2016; licensed under a Creative Commons Attribution (CC BY). (B) Three types of bioprinters. D. A. Foyt, et al. Adv. Healthc. Mater. 7, 1700939, 2018; licensed under a Creative Commons Attribution (CC BY).

Inkjet bioprinters dispense tiny droplets of bioink in picolitre range [3, 13-15]. For inkjet bioprinting, two commonly used methods are thermal and piezoelectric inkjet printing. Thermal inkjet bioprinters use an heating component in the print head to locally heat the bioink, causing vaporization which creates pressure pulses that propel droplets[13]. Piezoelectric inkjet printers use a piezoelectric component to generate acoustic waves in the printhead, breaking the bioink into droplets for ejection [16]. In general, inkjet printing has advantages of wide availability, low cost, while it also has significant disadvantages, such as the risk of exposing cells and biomaterials to high temperatures or sound frequencies, inconsistent droplet size and directionality and nozzle clogging[12].

Extrusion-based bioprinters utilize mechanical (driven by screw or piston) or pneumatic dispensing systems and can precisely move the printhead relative to the substrate on the x, y, and z axes [17]. Bioink is extruded into continuous, cylindrical

filaments of cells-capsulated materials in a controlled manner onto a substrate through an extrusion printhead. Overall, the extrusion-based bioprinting technique is capable of dispensing materials with a wide of rheological properties [18, 19]. Higher viscosities are often necessary for providing structural support for the printed products, while lower viscosities are typically better for preserving cell viability and function. This technique is particularly notable for its capability to print bioinks with varying cell densities and mechanical properties [20, 21].

Laser-assisted bioprinting utilizes the laser-induced forward transfer (LIFT) technique for printing bioinks in a drop-on-demand manner with potentially cell-level resolution. Laser pulse was used to vaporize the metal film and/or adjacent molecular layers of the bioink, creating bubbles that propel the bioink into droplets depositing onto the substrate [22, 23]. Laser-assisted bioprinting can precisely pattern bioink droplets to within 5.6 ± 2.5 μm of the intended design, enhancing control over cell density and 3D patterning [23, 24]. However, disadvantages include a low flow rate, high costs, metallic residues in the printed construct, and a limited printing size. These factors greatly restrict its application in bioprinting tissues or organs[12, 23].

2.2. Bioinks

During the bioprinting process, the biomaterial solution or mixture of multiple biomaterials, usually encapsulating the desired cell types, used for constructing tissue structures is termed bioink. [25]. Bioink is the crucial component of 3D bioprinting and it also has many vital requirements that need to be considered during the selection process as they significantly influence its capability to develop functional organs or tissue structures. The bioinks need to be biocompatible (not only non-toxic to surrounding cells or tissues but also maintain the cell viability) to fulfil the function of 3D bioprinted products. Rheological and mechanical properties are important to provide high resolution during printing and be mechanically stable after printing to maintain the structure of the bioprinted products. Hydrogel is becoming the gold standard material for bioinks due to its ability to hold great amounts of water while maintaining the structure [26, 27]. The high water content is essential for cell survival and also controls the permeation of nutrients and cellular products providing a microenvironment mimicking the natural extracellular matrix (ECM) which facilitates the adhesion, proliferation, differentiation, and migration of cells [26, 28-30]. Various natural and synthetic hydrogels with or without functional fillers have been used as a base structure encapsulating the cells for tissue deposition and to maintain cell morphology and function with varying degrees of success [31].

Natural hydrogels are derived from biological sources, such as bovine fibrinogen and rat tail collagen, and possess inherent biocompatibility and bioactivity. They closely mimic the natural ECM, providing a desirable microenvironment for cell activities. However, due to their natural origins, the composition and properties of these hydrogels may vary between batches[32, 33]. Common natural hydrogels used in formulating bioinks include alginate, collagen, gelatin, and cellulose. Alginate, a natural water-soluble material primarily sourced from brown seaweed and bacteria, is favored for its ionic crosslinking properties that allow for the creation of stable structures[34]. Collagen, the main structural protein found in the ECM of articular cartilage and meniscus, is isolated from various biological tissues and retains key signalling and adhesive biochemical cues. It is biodegradable by metalloproteases in the body and is noted for its excellent cross-species compatibility [35, 36]. Gelatin, a biodegradable polypeptide derived from the hydrolysis of collagen, is often mixed with natural or synthetic hydrogels to improve their biological properties and has been added to alginate to enhance its printability while preserving the viability of embedded cells for bioprinting[37, 38]. Cellulose, a major structural component of plants, and its derivative, hydroxypropyl methylcellulose (HPMC), a water-soluble non-ionic polymer, are commonly used in 3D bioprinting for tissue engineering and drug delivery[39, 40].

Synthetic hydrogels are valued for the reproducibility and tailorability of their chemical properties and characteristics [34]. Commonly used synthetic hydrogels in tissue engineering include polyethylene oxide (PEO), Pluronic F-127, modified cellulose, and their composites. PEO(CH_2CH_2O)n, a polymer of ethylene oxide monomers with molecular weights above 30,000 g/mol, is referred to as polyethylene glycol (PEG) when the molecular weight is below 30 kDa[41]. Due to its good biocompatibility and swelling properties, PEO is predominantly used in drug delivery applications[42]. Pluronic F127, also named Poloxamer 407, is a synthetic, amphiphilic copolymer approved by the FDA. Its amphiphilic nature allows self-assembling into small micelles in aqueous solutions, which are suitable for drug loading. Its thermogelling property enables F127 to encapsulate cells within its structure and supports cell adhesion to the defect site, facilitating tissue regeneration[43-45].

Functional fillers, such as ceramic nanoparticles, are added to bioinks to enhance the properties of the inks and the functions of printed products, including rheological properties, printability, mechanical strength, and bioactivity. For example, Laponite nanoclay (LP) is a commonly used bioactive filler and viscosity enhancer in bioinks due to its high efficiency in enhancing the viscosity, modulus and shear-thinning behavior of bioinks [46]. Hydroxyapatite (nHA), renowned for its role in bone tissue

engineering, closely resembles the inorganic component of human bone. This high chemical similarity results in a strong affinity for the host natural bone tissues, making it highly effective for reconstruction purposes [47, 48]. Bioactive glass, a type of bioceramic, is celebrated for its exceptional biocompatibility and ability to bond with bone and soft tissues, presenting significant properties of biocompatibility and osseointegration[49, 50].

The varying bioinks used for 3D bioprinting and their applications are summarized in Table 1

Table 1 Ink materials for bioprinting and their applications.

	Hydrogel matrix	Functional fillers	Cell type	Post-printing viability	Application	Ref
Natural hydrogel	3 wt% Alginate + 3 wt% methyl cellulose	6 wt% Laponite	Human chondrocytes and pre-osteoblasts	80%	Osteochondral tissue	51
	6% (w/w) sodium alginate+16% (w/w) gelatin	-	Human kidney fibroblasts	90%	Kidney tissue	52
	2.5 w/v% Alginate	2 w/v% nanoHA	Chick chondrocyte	86%	Calcified cartilage	53
	10 w/v% GelMA	-	Mouse fibroblast cell	90%	High viability tissue construct	54
	0.5% w/v alginate	2 w/v% nanocellulose	Human chondrocytes	86%	Cartilage	55
	4% w/v alginate+ 2% w/v collagen	-	Human breast cancer cells	90%	Breast cancer model	56
	5-10% w/v GelMA	1-3.5% w/v Laponite	Human PDAC cells	-	Pancreatic tissue	57
Synthetic hydrogel	20% w/v Poly(ethylene glycol dimethacrylate)	-	Human chondrocytes	95%	Cartilage	58
	25%w/v Pluronic F127	-	Mouse fibroblasts	80%	Osteochondral tissue	59
	2.5% w/v PVP	-	Human lung cell lines and lung fibroblasts	97%	Lung tissue	60
Composite hydrogel	1 w/v% Alginate + 5 w/v% poly(2-ethyl-2-oxazoline)	2 w/v% cellulose nanofibrils	Rat bone marrow-derived stem cells	90%	Cartilage	61
	30 w/v% F127 + 3 w/v% collagen	-	Human mesenchymal stem cells	88%	Cornea; Cartilage; Skin	62
	5 w/v% GelMA + 2 w/v% alginate + 1 w/v% PEG	2 w/v% Laponite	Human endothelial cells	95%	Vascularized tissues	46
	13 wt% F127 + 6 wt% alginate	-	Rat bone marrow stem cells	87%	Osteochondral	63
	6wt% polyvinyl alcohol + 18.2 wt% alginate	-	-	-	Bone tissue	64
	10% w/v PCL + collagen	-	Human colorectal cancer cell line	-	Colorectal cancer model	65
	2.5%GelMA + 2.5% Polyethylene glycol diacrylate (PEGDA)	-	Human melanoma cells	80%	Skin tissue	66

2.3. 3D bioprinting applications

With the advantages of precision, customization, scalability, and versatility, the 3D bioprinting technique is capable of creating tissue constructs and models that were previously unattainable with traditional methods. The diverse applications of 3D bioprinting in tissue engineering, regenerative medicine, cancer research, disease modelling, and illustrate the transformative potential of this technology. These applications are summarized in Table 1

In tissue and/or organ regeneration, the precision of 3D bioprinting allows for the creation of constructs with specific microarchitectures that enhance tissue functionality [67]. The ability to customize and precisely fabricate scaffolds that mimic the ECM enhances cell attachment, proliferation, and differentiation and is critical for developing effective biomedical devices and implants for clinical use [20]. The versatility in material uses and the capability in fabricating intricate structures are also crucial for developing multi-layered and vascularized tissues for creating functional tissue implants and advancing organ replacement therapies.

The customization capability enables the development of patient-specific in vitro models that mimic the morphological heterogeneity of human cancer tissues. This allows for more accurate drug response simulations and the development of personalized treatment strategies. [56]. For disease modeling and drug testing, the reproducibility and high-throughput capability of 3D bioprinting facilitate the creation of consistent and scalable models, essential for effective drug screening [51].

To adapt to dynamic physiological environments, stimuli-responsive materials are used in 3D bioprinting to enable shape or functional transformations, closely mimicking the dynamic behaviours of native tissues [68, 69]. This approach, known as 4D bioprinting, adds 'time' as a fourth dimension, allowing the bioprinted products not only to replicate the complex geometry of natural organs but also to adapt to dynamic environments or undergo maturation and evolution in a programmed manner[68, 70, 71].

Overall, 3D bioprinting, a pioneering field at the intersection of medicine, material science, engineering, and biology, holds immense promise for advancing medical research and clinical applications. Despite its potential and wide applications, it faces numerous challenges across technical, biological, and operational aspects. These include achieving high structural integrity of the printed products, maintaining the viability and functionality of cells, and ensuring reproducibility and reliability of bioprinting processes.

To overcome these obstacles, optimizing bioinks, print design and printing parameters and incorporating advanced printing modalities are crucial for enhancing precision customizability and reducing human error. Additionally, the ability to process and optimize data can significantly accelerate bioprinting development compared to the traditional trial-and-error methods, which are resource- and time-consuming [72, 73]. In response to these demands, Artificial Intelligence (AI) emerges as a critical tool. It addresses various challenges by enhancing the capabilities and impact of bioprinting technologies. AI can be integrated into various stages of the bioprinting workflow, processing vast amounts of data to accelerate and optimize designs, materials, and printing processes. This capability not only speeds up the development cycle but also introduces a level of precision difficult to achieve manually[74-76].

3. Artificial intelligence in 3D bioprinting

The term artificial intelligence (AI) was coined by John McCarthy and can be defined as the intelligence demonstrated by machines [77]. As the computational speed of machines has improved rapidly, the early approach of rule-based systems has been widely used to store, analyse and manipulate data [78]. The rule-based system consists of a set of rules, particularly if-then rules, coded through expert knowledge or learning from real data [79]. Classical AI leverages the rule-based system's approach with a more complex and nuanced knowledge base that represents the expertise of human specialists in specific domains [80]. Using rule-based algorithms and expert knowledge, classical AI provides a structured approach to reliable problem-solving and automation on specific tasks with explicit reasoning [81, 82]. The advent of machine learning (ML) methods marks another crucial shift in AI. It leverages learning systems that can process and learn from a large number of data and perform pattern recognition and predictive analytics on new data for complex decision-making processes and optimization. As ML does not rely on handcrafted features or explicit rules, it provides an alternative and powerful approach to completing complex tasks with new situations not directly covered by the original knowledge base, which can be challenging using the unaided human brain or traditional approaches [83-85]. ML is significantly influencing healthcare and biomedical applications such as diagnosis with medical images [86, 87], and recognizing a specific gene in a DNA sequence [88, 89].

Basic ML methods can be classified into two main categories: supervised and unsupervised machine learning according to task [88]. Unsupervised learning methods are trained with unlabeled data to discover hidden patterns or group the inputs without target variables [90, 91]. Examples of unsupervised learning include identifying latent

infectious diseases by mining social media data [92] and autonomous defect detection in laser powder bed 3D printing with anomaly detection techniques [93]. Supervised learning algorithms are trained with labelled data to establish the function that connects the inputs X to the unknown outputs Y and make predictions. It is currently the most widely used machine-learning method [91]. The function is based on the extrapolation of patterns discovered in the labelled input [94, 95]. The supervised learning method is widely used to solve classification and regression problems. Examples of classification problems include disease diagnosis [96] and risk gene identification [97].

In the 3D bioprinting field, ML algorithms have been used in major aspects including material selection, optimization of the model design and printing parameters, and *in situ* monitoring [75, 76, 98, 99]. The amount of data generated from these aspects is huge and the ML approach has demonstrated to be a prominent tool to overcome time-consuming, physics-based challenges efficiently [72, 73]. This can significantly accelerate the design-test cycle, reducing the time, resources and cost in the development of new biomaterials and printing techniques.

"Advancements in AI have substantially broadened its interdisciplinary applications, notably through the adoption of machine learning (ML) techniques in recent years [100, 101]. In 3D bioprinting, AI has been used across several stages of bioprinting including print design, bioink selection, and bioprinting process. Machine learning (ML) has experienced a surge in popularity and has been the focus of several review papers in recent years. It is even sometimes used interchangeably with AI. However, also as a part of AI, classical AI has not been well reviewed in the bioprinting field, although it has been playing a significant role in the foundational techniques of bioprinting. This review fills the gap in the literature by providing a systematic review of the full spectrum of AI in bioprinting, encompassing both classical AI and machine learning techniques. The schematics of how these two approaches of AI have been utilized in bioprinting are shown in Figure 3. This dual approach not only emphasizes the depth of AI's integration into bioprinting but also sets the stage for future advancements where both classical AI and machine learning can synergistically enhance bioprinting technologies.

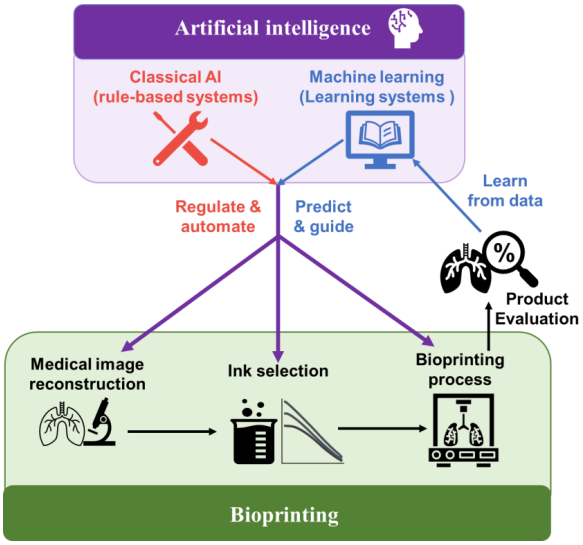

Figure 3 Schematics illustrating the use of artificial intelligence in 3D bioprinting. Both classical AI and learning systems of artificial intelligence have been integrated in different stages of bioprinting including print design, ink formulations and properties, and the bioprinting process.

3.1. Medical image reconstruction

The designing stage at the start of 3D bioprinting usually involves image acquisition from patients which guides the design of the 3D printing structure [102]. Raw imaging data of target tissues or organs is obtained with medical imaging technologies including magnetic resonance imaging (MRI), and computed tomography (CT) which generate slice-by-slice images of target tissues or organs. The subsequent step is the meticulous segmentation of these images, wherein specific regions of interest within the organ are delineated and distinguished from the surrounding tissue. The segmented data are then converted into computer-aided design (CAD) software, which facilitates the reconstruction of a digital 3D representation of the organ. This model serves as a blueprint for the generation printpath and printing parameters for the bioprinting process [103-105]. The accuracy of each step is critical to the quality and functionality of the printed structures. Traditional medical image segmentation and process methods are often time-consuming and error-prone [103]. Artificial intelligence has introduced automated segmentation algorithms and enhancement tools that significantly reduce manual input, increase efficiency, and minimize errors.

Classic AI has been used to improve and automate the processes of image enhancement and segmentation, medical image reconstruction and printpath

generation [106-108]. Bouzon, Albertini, Viana, Medeiros and Rodrigues [109] have employed a bio-inspired algorithm alongside computer vision and computer graphics techniques for medical image reconstruction, which is particularly challenging in unstructured scenes such as internal biological organs. The algorithms optimized image segmentation by minimizing entropy, detecting key points and mismatched point pairs in the images to extract and discard them respectively, which collectively enhanced the quality of reconstruction. Sainz-DeMena, García-Aznar, Pérez and Borau [106] have developed the im2mesh python library for the automation of transforming segmented slices into detailed 3D meshes, integrating scattered data through slice interpolation, and improving the usability and integration of these models into patient-specific simulations. The resultant 3D mesh has shown higher intersection over union (IoU) scores when comparing surfaces generated by established software like 3D Slicer. With the reconstructed 3D model, classic AI has also been used to generate reliable printpath autonomously. Nguyen, Phung and Bui [110] integrated computer-aided process planning systems and macro programming techniques to automate and enhance the generation of G-codes for CNC machining. With the recognition of the geometric features of the CAD model and the subsequent generation of G-code, this system has enhanced the flexibility customizability, and speed of the process.

As ML methods excel in pattern recognition and making predictions, it has been used for optimizing image segmentation for medical image reconstruction. Roth, Oda, Zhou, Shimizu, Yang, Hayashi, Oda, Fujiwara, Misawa and Mori [111] have developed cascaded FCNs for segmentation from CT images. It utilizes a two-stage, coarse-to-fine approach that allows for effective segmentation of complex anatomical structures across varying scales, from large organs to thin vessels. This approach refines the segmentation, particularly around the boundaries of smaller organs and vessels, and improves the mean Dice score significantly, demonstrating a substantial enhancement in the accuracy of segmentation. Chowa, Azam, Montaha, Bhuiyan and Jonkman [112] introduced a novel method that can transform traditional 2D ultrasound images into 3D meshes, capturing detailed geometrical features of breast tumours which are often lost in conventional imaging techniques by extracting clinically significant features from these 3D representations and utilizing a graph attention network.

3.2. Ink selection

The variety of available biomaterials for 3D bioprinting offers a diverse array of natural and synthetic polymers and functional fillers as shown in Table 1. Each material

comes with its unique set of physical, chemical, and biological characteristics. These properties, including viscosity, gelation behaviour, degradation rate and biocompatibility can profoundly influence the outcomes of 3D bioprinting. For instance, a bioink's rheological properties can affect its printability and resolution, while its biochemical attributes might determine cell-matrix interactions and tissue maturation. Given the myriad combinations and the interplay of these properties, developing the optimal ink formulation is extremely empirical and requires expert knowledge in various fields [113-115].

ML presents a groundbreaking approach to ink development with its capacity to sift through vast datasets and discern patterns that might be considered large and complex for humans [115, 116]. The printability of inks is a fundamental property for 3D printing as it can greatly influence the integration and function of printed implants [117]. It is evaluated by assessing the shape fidelity of printed products. ML has been utilized to forecast the printability of biomaterial formulations, aiding in the development of bioinks. Chen, Liu, Balabani, Hirayama and Huang [113] have used ML learning algorithms to predict printable biomaterial formulations for direct ink writing (DIW), an extrusion-based printing technique. The data used in their study consists of 210 ink formulations with two ink systems (hydrogel-based and polymer organic solution-based), 16 biomaterials, both natural and synthetic, and 4 solvents. The biomaterials include polymers of a range of molecular weights and properties and functional fillers with different sizes and functions. The inks were 3D printed into 4-layer lattice structures using DIW technique and their printability was assessed. The ML algorithms including decision tree, random forest, and deep learning have successfully predicted the printability of biomaterial formulations using their formulations with high accuracy (>88%) as shown in Figure 4 (A). In addition, a printability map of biomaterial composites can be generated using the trained ML algorithms to guide the ink design (Figure 4(B)). This study has opened the gate for using ML in guiding the selection of materials with a range of properties for DIW 3D printing, including hydrogels for bioprinting.

Nadernezhad and Groll [114] have used a random forest algorithm to predict the printability of hyaluronic acid-based hydrogel inks using their rheological properties. In addition, the importance of different rheological properties was quantitatively assessed and 13 critical rheological measurements that define the printability of hydrogel formulations have been identified (Figure 4 (D)). From a statistical perspective, the trained model predicts that a printable formulation should exhibit high yield viscosity and minimal plasticity before flowing. Additionally, the shift from

Newtonian to non-Newtonian flow characteristics should happen at comparatively low shear rates.

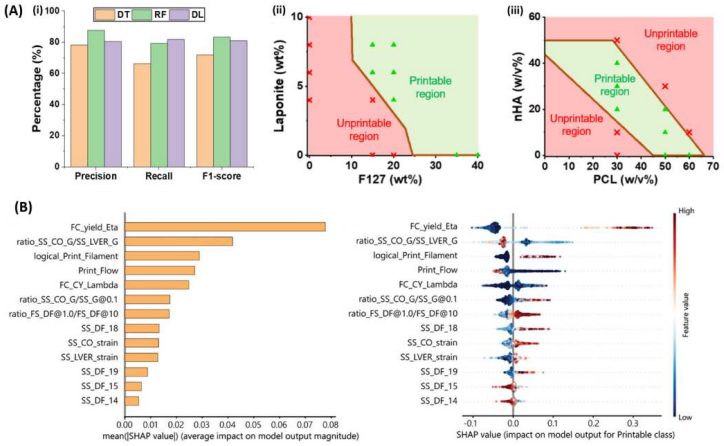

Figure 4. Machine learning in material selection for bioprinting. (A) Machine learning in predicting the printability of inks consisting of both hydrogel-based and polymer/organic solvent systems. (i) Evaluation metrics of accuracy, precision, recall, and F1 score of ML models in predicting printability. (ii) The predicted printability table of F127/Laponite hydrogel nanocomposite. (iii) hydroxyapatite nanoparticles loaded polycaprolactone polymer nanocomposite ink. Chen, et al., Research., 6**,** 0197. 2023; licensed under a Creative Commons Attribution (CC BY). (B) SHAP values of different features (rheological properties) of inks compare their contributions to the prediction on a global scale (left) and a local scale (right). A higher value indicates a higher contribution to the change in printability. Nadernezhad, et al., Adv. Sci., 9**,** 2202638. 2022; licensed under a Creative Commons Attribution (CC BY).

3.3. Printing process

3.3.1. AI-enabled *in situ* printing

The current bioprinting approach involves bioprinting a cellular tissue structure at the fabrication site which is then transferred to the surgery room for transplantation [12, 118]. Despite its great potential, intrinsic challenges of conventional 3D bioprinting exist which may hinder the fulfillment of its full potential. The bioprinting process is typically on a flat substrate, however, the defect site is often irregular and complicated leading to issues in achieving geometric alignment between the printed and target surfaces. The handling, transferring and implantation processes pose risks of damaging the micro- or macro-architectures of the mechanically weak bioprinted cellular structures. The risk of contamination during these processes is also a major concern [118-121].

In situ 3D bioprinting has emerged to address these challenges. It involves the deposition of bioinks directly on the defect site in a clinical setting for the regeneration

of tissues or organs with a minimally invasive route. This technique is capable of regenerating and reconstructing damaged tissues with non-planar surfaces or complex geometries. After printing, the human body acts as an "in vivo bioreactor," overseeing the post-printing development and maturation which eliminates the need to create an artificial microenvironment for the maturation of bioprinted products *in vitro* with bioreactors [118, 122]. Surface acquisition and print path planning are crucial for *in situ* printing. Properly determining the surface geometry ensures accurate deposition of material, and efficient print path planning ensures the printing process is optimized for speed, material use, and final product quality.

Classical AI systems have been used to acquire geometric information, create printing paths and incorporate intelligent printing systems. This has enabled *in situ* 3D printing on complex and non-planar surfaces [123]. In a review paper by Zhu, Ng, Park and McAlpine [123] these AI systems were categorized into open-loop, closed-loop and predictive AI systems. In open-loop AI systems, the target surface is static, and the geometry is prescribed to generate the print path. In a closed-loop AI system, a feedback-control system adapts the print path during the printing process allowing 3D printing on moving surfaces. A schematic showing the use of AI in 3D bioprinting is shown in Figure 3.

Open-loop 3D printing involves obtaining information about the target surface geometry before the printing process that is operated offline. Subsequently, AI can analyze this geometric data to design the printpath and ink deposition for *in situ* printing. Various imaging techniques, such as CT scanners [124], laser scanners [125] and structured-light scanners [126] have been used to acquire the 3D geometric data of the target surface.

Li, Shi, Ma, Jin, Wang, Liang, Cao, Wang and Jiang [127] used a robotic manipulator-based 3D printer for *in situ* printing in living animal models (Figure 5(A)). They performed 3D scanning to acquire the long segmental defect surface on the tibia of pigs for path planning with reverse engineering. Porous scaffold structures were printed on the defects in 12 minutes (Figure 5 (B)). Micro-CT scans revealed that the 3D bioprinting group exhibited a continuous cortical bone structure at the defect site after three months, whereas the control group displayed gaps and cavities. Histological analysis also showed improved morphology of the healed bone tissue in the 3D bioprinting group. This demonstrates the feasibility of using the robotic printer to repair large segmental bone defects. Zhou, Yang, Wang, Wu, Gu, Zhou, Liu, Yang, Tang, Ling, Wang and Zang [128] introduced a ferromagnetic soft catheter robot (FSCR) system for intelligent and minimally invasive bioprinting (Figure 5 (C)). The FSCR

utilizes magnetic actuation and can be remotely controlled, allowing for precise and automated printing of various materials with a small incision. The 3D surface of a living rat's liver was reconstructed using CT, and a printing path was defined on the upper surface of the liver. The FSCR successfully printed conductive hydrogel in a spiral pattern on the liver's surface in vivo within 70 seconds (Figure 5 (D)).

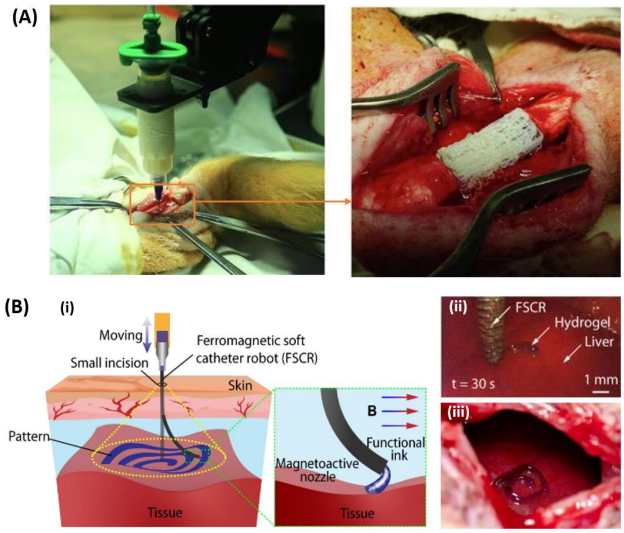

Figure 5. AI-guided *in situ* 3D bioprinting with open-loop system. (A) In situ bioprinting on a porcine long segmental bone defect using a robotic manipulator-based 3D printer. A porous bone scaffold was printed in the bone defect. Reproduced with permission from Li, et al. J. Adv. Res., 30, 75-84. (2021). Copyright 2021 Elsevier. (B) Schematics illustrate the minimally invasive printing process using a ferromagnetic soft catheter robot (FSCR) system. Functional inks, such as conducting polymers and living materials, are printed through the skin via a small incision. (ii) Minimally invasive printing of conductive hydrogel on the liver surface and (ii) resulting printed spiral pattern. (iii). Zhou, et al. Nat., Commun., 12, 5072. 2021; licensed under a Creative Commons Attribution (CC BY).

Closed-loop AI approach for *in situ* printing involves online 3D printing with real-time operational adaptations to changes including target surface motion and deformation, defects in printing and ink flows, and nozzle function [123]. This allows for improved printing quality through real-time correction and on-site printing on non-static surfaces. Zhao, Hu, Lin, Wang, Liu, Wang, Zhu and Xu [129] developed a closed-loop minimally invasive *in situ* bioprinting technique. This system includes a 7-axis bioprinting robot, a binary chromatic ring array (BCRA) marker for identifying the trocar, a vision system for capturing the trocar's movement, and a real-time control component (Figure 6(A)). The BCRA marker ensures precise positioning and poses estimation of the trocar,

while the bioprinting robot guides the end-effector through the trocar to carry out procedures within the small incision. The vision system captures the trocar's orientation, which is then used for real-time alignment and compensation of the printing end-effector's orientation. The system has printed hydrogels through an artificial skin on a porcine liver model with submillimetre accuracy, ensures minimal contact force at incisions and improved adaptability for intracorporal operations affected by respiration. (Figure 6 (B)). Zhu, Park and McAlpine [130] have developed a system capable of estimating the real-time movement of the target surface and adapt the printing process accordingly allowing *in situ* 3D printing on a moving lung model (Figure 6(C)). They used a stereo camera system to track fiducial markers on the tissue surface in a real-time shape basis model to estimate the deformation of the target surface. The system is capable of dynamically adapting the printing process from the real-time geometric states of the substrates. They successfully printed conductive hydrogel on a porcine lung and integrated it into a strain sensor with the ability of continuous spatial mapping of deformation. This adaptive 3D printing approach has the potential to enhance robot-assisted medical treatments and enable the printing of bioinks direct on and within the human for tissue regeneration or wearable electronics applications.

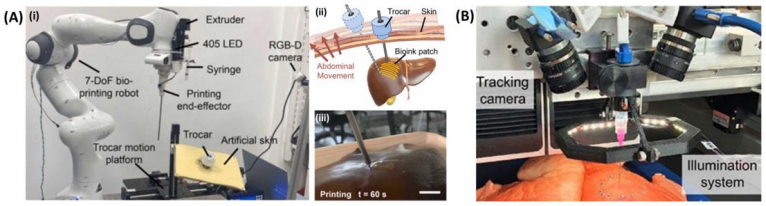

Figure 6. AI-guided i*n situ* 3D bioprinting with closed-loop system. (A) A closed-loop minimally invasive 3D bioprinting system. (i) Experiment setup of the system hardware. Reproduced with permission from Zhao, et al. Addit. Manuf. 73, 103701 (2023). Copyright 2023 Elsevier. (ii) Schematics of minimally invasive *in situ* printing on the surface of a porcine liver in respiration conditions. (iii) Printed hydrogel patch on a porcine liver with minimally invasive operation. (B) 3D printing of the conductive hydrogel layer on a lung model undergoing respiration motion. Zhu, et al. Sci. Adv. 6, eaba5575 2020; licensed under a Creative Commons Attribution (CC BY).

3.3.2. Optimization of printing parameters

Printing parameters involved in the printing process directly influence various aspects of the bioprinted products, such as structural integrity, resolution, and cell viability. These parameters include the speed of printing, temperature settings, extrusion rate, and layer thickness.

As ML methods excel in pattern recognition and making predictions, it has been used to process images of printed structures and assess the quality. Jin, Zhang, Shao and Gu [131] developed an anomaly detection system based on machine learning algorithms and layer-by-layer images of printed hydrogel lattice structures. Neural network (CNN) models were used in combination with advanced image processing techniques to distinguish and classify imperfections such as discontinuity, nonuniformity, and irregularity. This anomaly detection system has the potential to be integrated into the real-time correction of process parameters autonomously, enhancing printing quality.

The automation from classical AI techniques can be combined with the image processing capability of ML to achieve real-time adjustment in the printing process. Chen, Dong, Ruelas, Ye, He, Yao, Fu, Liu, Hu, Wu, Zhou, Li, Huang, Zhang and Zhou [132] have developed an artificial intelligence-assisted high-throughput printing-condition-screening system that can assess the printing quality of deposited filaments and adjust the printing parameters in real-time accordingly (Figure 7 (A)). 3D printed hydrogel patterns were imaged using a smartphone, and an AI-assisted image-analysis algorithm assessed the images in real-time and synergistically adjusted the printing parameters including printing pressure, speed, and distance, accordingly. Deep learning ML algorithm was used to analyze the acquired images and assess the shape fidelity of the filaments. Classical AI enables automated control systems that input the images to the ML algorithm and adjust the printing parameters with high throughput. The hydrogel scaffolds produced through the printing process demonstrated enhanced biological performance and proved to be highly effective in expediting the healing process of diabetic wounds.

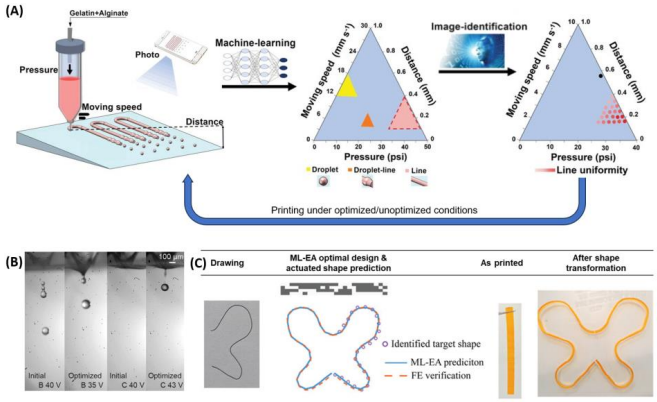

Figure 7. AI in optimization of the printing process. (A) AI-enabled high-throughput printing-condition-screening system capable of screening and adjusting the extrusion-based (bio)printing conditions with high throughput. Reproduced with permission from Chen, et al. Adv. Funct. Mater. 32, 2201843 (2022). Copyright 2022 Wiley-VCH. (B) Comparison of the inkjet printing of bio-inks with initial and optimized voltages. This optimization process has been shown to generate homogeneous primary droplets. Shi, et al., Engineering. 5, 586-593 2019; licensed under a Creative Commons Attribution (CC BY) license. (C) The process of using machine learning (ML) in 4D printing design involves several steps: recognizing the drawn profile as the target shape, applying the ML-EA (Machine Learning-Evolutionary Algorithm) for design optimization, generate grayscale slices from the optimal design, 3D printing, and expanding the printed structure for actuation. Reproduced with permission from Sun, et al. Adv. Funct. Mater. 32, 2109805 (2022). Copyright 2022 Wiley-VCH.

Besides extrusion-based printing, ML has also been used to assess droplet forming of drop-on-demand printing to optimize the printing parameters. Shi, Song, Song and Lu [133] have developed fully connected neural networks to optimize the inkjet printing parameters. By solving a single-objective optimization problem, they determined the optimal voltage for each bio-ink, which was then successfully used to print a single primary droplet. A hybrid multi-subgradient descent bundle method with an adaptive learning rate algorithm (HMSGDBA) was used to search for the Pareto-optimal set for a multi-objective optimization problem. The optimized parameters obtained through the proposed method improved the printing precision and stability as shown in (Figure 7 (B)).

ML has been used to assess and optimize the shape actuation for 4D printing. Sun, Yue, Yu, Shao, Peng, Zhou, Demoly, Zhao and Qi [134] have developed machine learning and evolutionary algorithms in the design of 4D printing active composite structures (Figure 7 (C)). The goal is to optimize a design to achieve a target shape transformation. The approach involves training a recurrent neural network (RNN) model using finite element simulations for predicting the shape change and using an

evolutionary algorithm (EA) empowered with machine learning to find the optimal design. The ML-EA algorithms demonstrate high efficiency in designing 4D-printed active composites for achieving multiple target shapes. The authors propose a new paradigm that integrates computer vision algorithms with ML-EA, streamlining the design and 4D printing process to enable the rapid 4D printing of beams from hand-drawn lines. This ML-EA approach achieves high accuracy, is computationally faster than finite element simulations, and can be applied to different material and fabrication systems with varying active strain mechanisms.

As both materials and printing parameters contribute to the shape fidelity of the printed products, ML has been utilized to predict the desired ink formulations and printing parameters collectively. In the study conducted by Kim, Lee, Han, Kang, Park, Kim, Lee, Kim, Na, Oh, Bang, Jang, Kim, Park, Shin and Jung [135], the Gaussian process regression machine learning model was used to optimize the hydrogel concentration and printing parameters for 3D printing functionalized alginate hydrogel for diabetic wound dressing. Using ML, the team predicted optimal hydrogel concentrations and printing parameters to achieve desirable printability. The model's accuracy reached an R^2 value of 82%. This predictive modelling enabled the precise fabrication of dressings that protect the wounds from mechanical deformations.

4. Conclusions and Future Perspective

The burgeoning field of 3D bioprinting has made substantial strides in recent years. It integrates advances in biomaterials, printing technologies, and computational methods to push the boundaries of tissue engineering and regenerative medicine. While advancements have been made, several challenges persist in bioprinting. Currently, it struggles to replicate the complex micro- and macro-architecture and mechanical and biochemical cues of native tissues and ensure the cell activities and functionality of printed tissues over time [18, 136, 137].

The interplay of AI with 3D bioprinting is poised to revolutionize this landscape by surmounting the current challenges of 3D bioprinting and unlocking new possibilities. Comprising both classical AI and machine learning approaches, AI is capable of processing and interpreting large datasets generated from high throughput experiments and has pushed advances in 3D bioprinting by generating printpaths for printing on complex surfaces, selecting bioink materials and refining designs and printing parameters. The classical AI approach has been used to regulate and automate different processes for bioprionting. In the print design phase, it has been used to automate the medical image processing and printpath generation based on

medical image reconstruction. In the printing process, it allows *in situ* bioprinting by automating the movement of the nozzle based on the complex surface geometry of the substrate and *in situ* monitoring and adaptation of the printing parameters. The machine learning approach excels in finding patterns and making predictions from large amounts of data and guides the bioprinting process including image segmentation, bioink selection and parameter optimization.

In the future, the importance of AI in bioprinting will continue to grow. As the field of bioprinting advances, it will inevitably become more complex, with an increasing accumulation of data throughout its processes. Simultaneously, as AI technology evolves, improvements in computational speed and robustness are expected. This advancement will undoubtedly magnify the role of AI in bioprinting, especially in managing and optimizing the vast datasets that inform printing design, bioink selection and printing parameters.

AI is currently an isolated computing block in the bioprinting process. Looking ahead, integrating concepts from the latest advancements, such as digital twins and big data, could further integrate AI into bioprinting [138]. The creation of digital twins of human organs, informed by vast arrays of big data derived from medical imaging, bioink formulations, printing parameters and assessments of printed products, will enable AI systems to simulate and predict the outcomes of bioprinting processes with high accuracy. Additionally, this predictive capacity, rooted in comprehensive data analysis, facilitates the ability of AI-enabled bioprinting systems to become fully autonomous in printing and evolving themselves. Such systems would be capable of identifying tissue defects from medical imaging, initiating print design, selecting appropriate bioinks, and executing printing with optimized parameters autonomously. This level of automation would not only minimize human errors but also allow surgeons and clinicians to conduct or supervise complex bioprinting processes without expert knowledge of bioprinting. In addition, the use of ML for bioprinting is currently focused on achieving adequate structure integrity, by selecting bioinks with high printability and optimized printing parameters. While the structure integrity is fundamental for 3D bioprinting, other factors such as mechanical properties, cell viability, proliferation and differentiation are also vital for the function of the bioprinted products [117, 139-141]. By integrating big data, which encompasses these diverse aspects, along with the concept of digital twins, bioprinting can be significantly enhanced across various dimensions of the process.

In conclusion, as AI technology advances in capability and sophistication, its integration into bioprinting becomes increasingly essential. AI is set to play a pivotal

role not only in enhancing existing processes but also in driving innovation within the field. By continuing to utilize AI, the bioprinting field can look forward to overcoming current limitations and unlocking new potentials in the creation of complex, functional, and patient-specific tissues.

Acknowledgements

B.Z. would like to thank Royal Society Research Grant for supporting the research work and collaborations.

Declarations

There are no conflicts to declare.

References

1. P. Bajaj, R. M. Schweller, A. Khademhosseini, J. L. West and R. Bashir, Annual review of biomedical engineering **16**, 247-276 (2014).

2. J. W. Nichol and A. Khademhosseini, Soft matter **5** (7), 1312-1319 (2009).

3. R. F. Pereira and P. J. Bártolo, Journal of Applied Polymer Science **132** (48) (2015).

4. C. Yu, K. L. Miller, J. Schimelman, P. Wang, W. Zhu, X. Ma, M. Tang, S. You, D. Lakshmipathy and F. He, Biomaterials **258**, 120294 (2020).

5. X. Ma, X. Qu, W. Zhu, Y.-S. Li, S. Yuan, H. Zhang, J. Liu, P. Wang, C. S. E. Lai and F. Zanella, Proceedings of the National Academy of Sciences **113** (8), 2206-2211 (2016).

6. P. Jain, H. Kathuria and N. Dubey, Biomaterials **287**, 121639 (2022).

7. H. Cui, M. Nowicki, J. P. Fisher and L. G. Zhang, Advanced healthcare materials **6** (1), 10.1002/adhm.201601118 (2017).

8. H.-W. Kang, S. J. Lee, I. K. Ko, C. Kengla, J. J. Yoo and A. Atala, Nature Biotechnology **34** (3), 312-319 (2016).

9. N. J. Braun, R. M. Galaska, M. E. Jewett and K. A. Krupa, Nanomaterials **11** (7), 1807 (2021).

10. K. Duval, H. Grover, L.-H. Han, Y. Mou, A. F. Pegoraro, J. Fredberg and Z. Chen, Physiology **32** (4), 266-277 (2017).

11. A. Goyanes, M. Kobayashi, R. Martínez-Pacheco, S. Gaisford and A. W. Basit, International journal of pharmaceutics **514** (1), 290-295 (2016).

12. S. V. Murphy and A. Atala, Nature Biotechnology **32** (8), 773-785 (2014).

13. K. Hölzl, S. Lin, L. Tytgat, S. Van Vlierberghe, L. Gu and A. Ovsianikov, Biofabrication **8** (3), 032002 (2016).

14. T. Xu, H. Kincaid, A. Atala and J. J. Yoo, Journal of Manufacturing Science and Engineering, Transactions of the ASME **130** (2), 0210171-0210175 (2008).

15. X. Cui, T. Boland, D. D. D'Lima and M. K. Lotz, Recent Pat Drug Deliv Formul **6** (2), 149-155 (2012).

16. E. Tekin, P. J. Smith and U. S. Schubert, Soft Matter **4** (4), 703-713 (2008).

17. S. Muthusamy, S. Kannan, M. Lee, V. Sanjairaj, W. F. Lu, J. Y. H. Fuh, G. Sriram and T. Cao, Biotechnol Bioeng **118** (8), 3150-3163 (2021).

18. A. Schwab, R. Levato, M. D'Este, S. Piluso, D. Eglin and J. Malda, Chemical Reviews **120** (19), 11028-11055 (2020).

19. H. Chen, T. Stampoultzis, A. Papadopoulou, S. Balabani and J. Huang, Orthopaedic Proceedings **103-B** (SUPP_2), 96-96 (2021).

20. S. You, Y. Xiang, H. H. Hwang, D. B. Berry, W. Kiratitanaporn, J. Guan, E. Yao, M. Tang, Z. Zhong, X. Ma, D. Wangpraseurt, Y. Sun, T.-y. Lu and S. Chen, Science Advances **9** (8), eade7923 (2023).

21. H. Chen, J. Khong and J. Huang, Orthopaedic Proceedings **103-B** (SUPP_16), 74-74 (2021).

22. B. Guillotin, A. Souquet, S. Catros, M. Duocastella, B. Pippenger, S. Bellance, R. Bareille, M. Rémy, L. Bordenave, J. Amédée and F. Guillemot, Biomaterials **31** (28), 7250-7256 (2010).

23. V. Keriquel, H. Oliveira, M. Rémy, S. Ziane, S. Delmond, B. Rousseau, S. Rey, S. Catros, J. Amédée, F. Guillemot and J.-C. Fricain, Sci Rep **7** (1), 1778 (2017).

24. N. R. Schiele, D. B. Chrisey and D. T. Corr, Tissue Eng Part C Methods **17** (3), 289-298 (2011).

25. P. S. Gungor-Ozkerim, I. Inci, Y. S. Zhang, A. Khademhosseini and M. R. Dokmeci, Biomaterials science **6** (5), 915-946 (2018).

26. B. V. Slaughter, S. S. Khurshid, O. Z. Fisher, A. Khademhosseini and N. A. Peppas, Advanced Materials **21** (32‐33), 3307-3329 (2009).

27. B. Choi, S. Kim, B. Lin, B. M. Wu and M. Lee, ACS Applied Materials & Interfaces **6** (22), 20110-20121 (2014).

28. I. Gibas and H. Janik, Chem. Chem. Technol. **4**, 297-304 (2010).

29. M. Yazdimamaghani, D. Vashaee, S. Assefa, K. Walker, S. Madihally, G. Köhler and L. Tayebi, Journal of biomedical nanotechnology **10**, 911-931 (2014).

30. S. Van Vlierberghe, P. Dubruel and E. Schacht, Biomacromolecules **12** (5), 1387-1408 (2011).

31. D.-J. Cornelissen, A. Faulkner-Jones and W. Shu, Current Opinion in Biomedical Engineering **2**, 76-82 (2017).

32. N. Chirani, L. H. Yahia, L. Gritsch, F. Motta, S. Chirani and S. Farè, Journal of Biomedical Sciences **Vol. 4**, 13-23 (2015).

33. T. McDonagh, B. Zhang and S. Qi, 3D Printing of Pharmaceutical and Drug Delivery Devices: Progress from Bench to Bedside, 1 (2024).

34. J. L. Drury and D. J. Mooney, Biomaterials **24** (24), 4337-4351 (2003).

35. S. Critchley and D. Kelly, Journal of 3D Printing in Medicine **1**, 269-290 (2017).

36. L. B. Rocha, G. Goissis and M. A. Rossi, Biomaterials **23** (2), 449-456 (2002).

37. J. H. Y. Chung, S. Naficy, Z. Yue, R. Kapsa, A. Quigley, S. E. Moulton and G. G. Wallace, Biomaterials Science **1** (7), 763-773 (2013).

38. H. Chen, G. Gonnella, J. Huang and L. Di-Silvio, Biomimetics **8** (1), 87 (2023).

39. P. Zarmpi, T. Flanagan, E. Meehan, J. Mann and N. Fotaki, European Journal of Pharmaceutics and Biopharmaceutics **111**, 1-15 (2017).

40. B. Zhang, X. Y. Teoh, J. Yan, A. Gleadall, P. Belton, R. Bibb and S. Qi, International Journal of Pharmaceutics **625**, 122140 (2022).

41. J. Herzberger, K. Niederer, H. Pohlit, J. Seiwert, M. Worm, F. R. Wurm and H. Frey, Chemical Reviews **116** (4), 2170-2243 (2016).

42. L. Viidik, D. Seera, O. Antikainen, K. Kogermann, J. Heinämäki and I. Laidmäe, European Polymer Journal **120**, 109206 (2019).

43. Y. Liu, S. Fu, L. Lin, Y. Cao, X. Xie, H. Yu, M. Chen and H. Li, Int J Nanomedicine **12**, 2635-2644 (2017).

44. H. H. Bearat and B. L. Vernon, in *Injectable Biomaterials*, edited by B. Vernon (Woodhead Publishing, 2011), pp. 263-297.

45. I. M. A. Diniz, C. Chen, X. Xu, S. Ansari, H. H. Zadeh, M. M. Marques, S. Shi and A. Moshaverinia, Journal of Materials Science: Materials in Medicine **26** (3), 153 (2015).

46. Z. Ma, H. He, C. Deng, Y. Ren, D. Lu, W. Li, X. Sun, W. Wang, Y. Zhang, Y. Xu, X. Zhou, L. Zhou, J. Lin, T. Li, T. Wu and J. Wang, Composites Part B: Engineering **229**, 109399 (2022).

47. B. Zhang, A. K. Nguyen, R. J. Narayan and J. Huang, Journal of the American Ceramic Society **105** (3), 1821-1840 (2022).

48. Y. Kim, E.-J. Lee, A. V. Davydov, S. Frukhtbeyen, J. E. Seppala, S. Takagi, L. Chow and S. Alimperti, Biomedical Materials **16** (4), 045002 (2021).

49. H. Zhou and J. Lee, Acta Biomaterialia **7** (7), 2769-2781 (2011).

50. S. Heid and A. R. Boccaccini, Acta Biomaterialia **113**, 1-22 (2020).

51. D. Kilian, S. Cometta, A. Bernhardt, R. Taymour, J. Golde, T. Ahlfeld, J. Emmermacher, M. Gelinsky and A. Lode, Biofabrication **14** (1), 014108 (2022).

52. H. Herrada-Manchón, L. Celada, D. Rodríguez-González, M. A. Fernandez, E. Aguilar and M.-D. Chiara, Materials Science and Engineering: C **128**, 112357 (2021).

53. F. You, X. Chen, D. M. L. Cooper, T. Chang and B. F. Eames, Biofabrication **11** (1), 015015 (2019).

54. L. E. Bertassoni, J. C. Cardoso, V. Manoharan, A. L. Cristino, N. S. Bhise, W. A. Araujo, P. Zorlutuna, N. E. Vrana, A. M. Ghaemmaghami, M. R. Dokmeci and A. Khademhosseini, Biofabrication **6** (2), 024105 (2014).

55. K. Markstedt, A. Mantas, I. Tournier, H. Martínez Ávila, D. Hagg and P. Gatenholm, Biomacromolecules **16** (5), 1489-1496 (2015).

56. J. Han, S. Jeon, M. K. Kim, W. Jeong, J. J. Yoo and H.-W. Kang, Biofabrication **14** (3), 034102 (2022).

57. N. R. de Barros, A. Gomez, M. Ermis, N. Falcone, R. Haghniaz, P. Young, Y. Gao, A.-F. Aquino, S. Li and S. Niu, Biofabrication (2023).

58. X. Cui, K. Breitenkamp, M. G. Finn, M. Lotz and D. D. D'Lima, Tissue engineering. Part A **18** (11-12), 1304-1312 (2012).

59. E. Gioffredi, M. Boffito, S. Calzone, S. M. Giannitelli, A. Rainer, M. Trombetta, P. Mozetic and V. Chiono, Procedia CIRP **49**, 125-132 (2016).

60. W. L. Ng, T. C. Ayi, Y.-C. Liu, S. L. Sing, W. Y. Yeong and B.-H. Tan, International Journal of Bioprinting **7** (2) (2021).

61. S. A. Wilson, L. M. Cross, C. W. Peak and A. K. Gaharwar, ACS Applied Materials & Interfaces **9** (50), 43449-43458 (2017).

62. K. K. Moncal, V. Ozbolat, P. Datta, D. N. Heo and I. T. Ozbolat, Journal of Materials Science: Materials in Medicine **30** (5), 55 (2019).

63. J. Armstrong, M. Burke, B. Carter, S. Davis and A. Perriman, Advanced Healthcare Materials **5**, 1681-1681 (2016).

64. Y. Luo, G. Luo, M. Gelinsky, P. Huang and C. Ruan, Materials Letters **189**, 295-298 (2017).

65. H. Chen, Y. Cheng, X. Wang, J. Wang, X. Shi, X. Li, W. Tan and Z. Tan, Theranostics **10** (26), 12127 (2020).

66. S. Sang, X. Wang, J. Duan, Y. Cao, Z. Shen, L. Sun, Q. Duan and Z. Liu, Biotechnology and Bioengineering (2023).

67. L. E. Bertassoni, J. C. Cardoso, V. Manoharan, A. L. Cristino, N. S. Bhise, W. A. Araujo, P. Zorlutuna, N. E. Vrana, A. M. Ghaemmaghami, M. R. Dokmeci and A. Khademhosseini, Biofabrication **6** (2), 024105-024105 (2014).

68. Z. Wan, P. Zhang, Y. Liu, L. Lv and Y. Zhou, Acta Biomaterialia **101**, 26-42 (2020).

69. Y.-C. Li, Y. S. Zhang, A. Akpek, S. R. Shin and A. Khademhosseini, Biofabrication **9** (1), 012001 (2016).

70. D. Raviv, W. Zhao, C. McKnelly, A. Papadopoulou, A. Kadambi, B. Shi, S. Hirsch, D. Dikovsky, M. Zyracki, C. Olguin, R. Raskar and S. Tibbits, Sci Rep **4** (1), 7422 (2014).

71. B. Gao, Q. Yang, X. Zhao, G. Jin, Y. Ma and F. Xu, Trends in Biotechnology **34** (9), 746-756 (2016).

72. G. D. Goh, S. L. Sing and W. Y. Yeong, Artificial Intelligence Review **54** (1), 63-94 (2021).

73. M. Rezapour Sarabi, M. M. Alseed, A. A. Karagoz and S. Tasoglu, Biosensors **12** (7), 491 (2022).

74. Y. Shi, Y. Zhang, S. Baek, W. De Backer and R. Harik, Computer-Aided Design and Applications **15** (6), 941-952 (2018).

75. Z. Gan, H. Li, S. J. Wolff, J. L. Bennett, G. Hyatt, G. J. Wagner, J. Cao and W. K. Liu, Engineering **5** (4), 730-735 (2019).

76. T. Erps, M. Foshey, M. K. Luković, W. Shou, H. H. Goetzke, H. Dietsch, K. Stoll, B. von Vacano and W. Matusik, Science Advances **7** (42), eabf7435 (2021).

77. J. McCarthy, Automata studies, 177-181 (1956).

78. R. Karthikeyan, P. Geetha and E. Ramaraj, presented at the 2019 3rd International Conference on Computing and Communications Technologies (ICCCT), 2019 (unpublished).

79. H. Liu, A. Gegov and M. Cocea, Granular Computing **1** (4), 259-274 (2016).

80. A. Asemi, A. Ko and M. Nowkarizi, Library Hi Tech **39**, 412-434 (2021).

81. R. L. Cechner and C. A. Sutheimer, Journal of Analytical Toxicology **14** (5), 280-284 (1990).

82. L. Wang, J. Yan, L. Mu and L. Huang, WIREs Data Mining and Knowledge Discovery **10** (5), e1371 (2020).

83. A. I. Georgevici and M. Terblanche, Intensive Care Medicine **45** (5), 712-714 (2019).

84. S. Shane, G. Jemin and B. Carl, presented at the Proc.SPIE, 2022 (unpublished).

85. N. M. J. Kumari and K. K. V. Krishna, presented at the 2018 International Conference on Current Trends towards Converging Technologies (ICCTCT), 2018 (unpublished).

86. R. Arnaout, L. Curran, Y. Zhao, J. C. Levine, E. Chinn and A. J. Moon-Grady, Nature Medicine **27** (5), 882-891 (2021).

87. M. A. Badgeley, J. R. Zech, L. Oakden-Rayner, B. S. Glicksberg, M. Liu, W. Gale, M. V. McConnell, B. Percha, T. M. Snyder and J. T. Dudley, npj Digital Medicine **2** (1), 31 (2019).

88. K.-H. Yu, A. L. Beam and I. S. Kohane, Nature Biomedical Engineering **2** (10), 719-731 (2018).

89. A. Esteva, A. Robicquet, B. Ramsundar, V. Kuleshov, M. DePristo, K. Chou, C. Cui, G. Corrado, S. Thrun and J. Dean, Nature Medicine **25** (1), 24-29 (2019).

90. S. Bashir, U. Qamar and F. H. Khan, Journal of Biomedical Informatics **59**, 185-200 (2016).

91. M. I. Jordan and T. M. Mitchell, Science **349** (6245), 255-260 (2015).

92. S. Lim, C. S. Tucker and S. Kumara, Journal of Biomedical Informatics **66**, 82-94 (2017).

93. L. Scime and J. Beuth, Additive Manufacturing **19**, 114-126 (2018).

94. J. Schmidt, M. R. G. Marques, S. Botti and M. A. L. Marques, npj Computational Materials **5** (1), 83 (2019).

95. M. W. Libbrecht and W. S. Noble, Nature Reviews Genetics **16** (6), 321-332 (2015).

96. A. Kleppe, O.-J. Skrede, S. De Raedt, K. Liestøl, D. J. Kerr and H. E. Danielsen, Nature Reviews Cancer **21** (3), 199-211 (2021).

97. S. Cogill and L. Wang, Bioinformatics **32** (23), 3611-3618 (2016).

98. C. Yu and J. Jiang, International Journal of Bioprinting **6** (2020).

99. A. F. Bonatti, G. Vozzi and C. De Maria, Biofabrication **16** (2), 022001 (2024).

100. M. Krenn, R. Pollice, S. Y. Guo, M. Aldeghi, A. Cervera-Lierta, P. Friederich, G. dos Passos Gomes, F. Häse, A. Jinich, A. Nigam, Z. Yao and A. Aspuru-Guzik, Nature Reviews Physics **4** (12), 761-769 (2022).

101. R. Kusters, D. Misevic, H. Berry, A. Cully, Y. Le Cunff, L. Dandoy, N. Díaz-Rodríguez, M. Ficher, J. Grizou, A. Othmani, T. Palpanas, M. Komorowski, P. Loiseau, C. Moulin Frier, S. Nanini, D. Quercia, M. Sebag, F. Soulié Fogelman, S. Taleb, L. Tupikina, V. Sahu, J.-J. Vie and F. Wehbi, Frontiers in Big Data **3** (2020).

102. I. T. Ozbolat and M. Hospodiuk, Biomaterials **76**, 321-343 (2016).

103. L. Ma, S. Yu, X. Xu, S. Moses Amadi, J. Zhang and Z. Wang, Materials Today Bio **23**, 100792 (2023).

104. J. Lee, H. Lee, E.-J. Jin, D. Ryu and G. H. Kim, npj Regenerative Medicine **8** (1), 18 (2023).

105. B. Zhang, T. McDonagh, J. Yan, A. Glendale, R. Bib, P. Belton and S. Qi, 3D Printing of Pharmaceutical and Drug Delivery Devices: Progress from Bench to Bedside, 29 (2024).

106. D. Sainz-DeMena, J. M. García-Aznar, M. Á. Pérez and C. Borau, Applied Sciences **12** (22), 11557 (2022).

107. N. Byrne, M. Velasco Forte, A. Tandon, I. Valverde and T. Hussain, JRSM Cardiovascular Disease **5**, 2048004016645467 (2016).

108. J. Matthew, A. Uus, L. De Souza, R. Wright, A. Fukami-Gartner, G. Priego, C. Saija, M. Deprez, A. E. Collado, J. Hutter, L. Story, C. Malamateniou, K. Rhode, J. Hajnal and M. A. Rutherford, BMC Medical Imaging **24** (1), 52 (2024).

109. M. Bouzon, G. Albertini, G. Viana, G. Medeiros and P. S. Rodrigues, presented at the 2019 XV Workshop de Visão Computacional (WVC), 2019 (unpublished).

110. T. K. Nguyen, L. X. Phung and N.-T. Bui, Machines **8** (4), 61 (2020).

111. H. R. Roth, H. Oda, X. Zhou, N. Shimizu, Y. Yang, Y. Hayashi, M. Oda, M. Fujiwara, K. Misawa and K. Mori, Computerized Medical Imaging and Graphics **66**, 90-99 (2018).

112. S. S. Chowa, S. Azam, S. Montaha, M. R. I. Bhuiyan and M. Jonkman, Journal of Imaging Informatics in Medicine (2024).

113. H. Chen, Y. Liu, S. Balabani, R. Hirayama and J. Huang, Research **6**, 0197 (2023).

114. A. Nadernezhad and J. Groll, Advanced Science **9** (29), 2202638 (2022).

115. M. Elbadawi, H. Li, S. Sun, M. E. Alkahtani, A. W. Basit and S. Gaisford, Applied Materials Today **36**, 102061 (2024).

116. J. G. Greener, S. M. Kandathil, L. Moffat and D. T. Jones, Nature Reviews Molecular Cell Biology **23** (1), 40-55 (2022).

117. C. Mota, S. Camarero-Espinosa, M. B. Baker, P. Wieringa and L. Moroni, Chemical Reviews (2020).

118. S. Singh, D. Choudhury, F. Yu, V. Mironov and M. W. Naing, Acta Biomaterialia **101**, 14-25 (2020).

119. Y. Wu, D. J. Ravnic and I. T. Ozbolat, Trends in Biotechnology **38** (6), 594-605 (2020).

120. Z. Zhu, D. W. H. Ng, H. S. Park and M. C. McAlpine, Nature Reviews Materials (2020).

121. M. T. Thai, P. T. Phan, H. A. Tran, C. C. Nguyen, T. T. Hoang, J. Davies, J. Rnjak-Kovacina, H.-P. Phan, N. H. Lovell and T. N. Do, Advanced Science **n/a** (n/a), 2205656 (2023).

122. M. Wang, J. He, Y. Liu, M. Li and Z. Jin, International Journal of Bioprinting **1** (2015).

123. Z. Zhu, D. W. H. Ng, H. S. Park and M. C. McAlpine, Nature Reviews Materials **6** (1), 27-47 (2021).

124. D. L. Cohen, J. I. Lipton, L. J. Bonassar and H. Lipson, Biofabrication **2** (3), 035004 (2010).

125. X. Zhao, Y. Pan, C. Zhou, Y. Chen and C. C. L. Wang, Journal of Manufacturing Processes **15** (4), 432-443 (2013).

126. L. Li, F. Yu, J. Shi, S. Shen, H. Teng, J. Yang, X. Wang and Q. Jiang, Sci Rep **7** (1), 9416 (2017).

127. L. Li, J. Shi, K. Ma, J. Jin, P. Wang, H. Liang, Y. Cao, X. Wang and Q. Jiang, Journal of Advanced Research **30**, 75-84 (2021).

128. C. Zhou, Y. Yang, J. Wang, Q. Wu, Z. Gu, Y. Zhou, X. Liu, Y. Yang, H. Tang, Q. Ling, L. Wang and J. Zang, Nature Communications **12** (1), 5072 (2021).

129. W. Zhao, C. Hu, S. Lin, Y. Wang, L. Liu, Z. Wang, Y. Zhu and T. Xu, Additive Manufacturing **73**, 103701 (2023).

130. Z. Zhu, H. S. Park and M. C. McAlpine, Science Advances **6** (25), eaba5575 (2020).

131. Z. Jin, Z. Zhang, X. Shao and G. X. Gu, ACS Biomaterials Science & Engineering **9** (7), 3945-3952 (2023).

132. B. Chen, J. Dong, M. Ruelas, X. Ye, J. He, R. Yao, Y. Fu, Y. Liu, J. Hu, T. Wu, C. Zhou, Y. Li, L. Huang, Y. S. Zhang and J. Zhou, Advanced Functional Materials **32** (38), 2201843 (2022).

133. J. Shi, J. Song, B. Song and W. F. Lu, Engineering **5** (3), 586-593 (2019).

134. X. Sun, L. Yue, L. Yu, H. Shao, X. Peng, K. Zhou, F. Demoly, R. Zhao and H. J. Qi, Advanced Functional Materials **32** (10), 2109805 (2022).

135. N. Kim, H. Lee, G. Han, M. Kang, S. Park, D. E. Kim, M. Lee, M.-J. Kim, Y. Na, S. Oh, S.-J. Bang, T.-S. Jang, H.-E. Kim, J. Park, S. R. Shin and H.-D. Jung, Advanced Science **10** (17), 2300816 (2023).

136. L. Faber, A. Yau and Y. Chen, Biofabrication **16** (1), 012001 (2024).

137. B. Zhang, M. Morgan, X. Y. Teoh, R. Mackay, S. Ermler and R. Narayan, Journal of Applied Physics **135** (14) (2024).

138. A. Jia, C. Chee Kai and M. Vladimir, IJB **7** (1), 342 (2021).

139. S. Derakhshanfar, R. Mbeleck, K. Xu, X. Zhang, W. Zhong and M. Xing, Bioact Mater **3**, 144-156 (2018).

140. H.-Q. Xu, J.-C. Liu, Z.-Y. Zhang and C.-X. Xu, Military Medical Research **9** (1), 70 (2022).

141. B. Zhang, Medical Engineering & Physics, 104173 (2024).